Hyperfine anomaly in Be isotopes and the neutron spatial distribution; a three-cluster model for ^{9}Be.

Y. L. Parfenova* and Ch. Leclercq-Willain†
Physique Nucléaire Théorique et Physique Mathématique, CP229, Université Libre de Bruxelles B 1050 Brussels, Belgium.
(Dated: February 9, 2008)

The study of the hyperfine (hfs) anomaly in neutron rich nuclei can give a very specific and unique way to study the neutron distribution and the clustering structure. We study the sensitivity of the hfs anomaly to the clustering effects in the ^{9}Be isotope using two different nuclear wave functions obtained in the three-cluster ($\alpha+\alpha+n$) model. The results are compared to those obtained for ^{9,11}Be in a two-body core + neutron model to examine whether the hfs anomaly is sensitive to a halo structure in ^{11}Be.

PACS numbers: 32.10.Fn; 21.10.Gv; 21.60.Gx; 21.10.Ky

I. INTRODUCTION

The study of the hyperfine (hfs) anomaly in neutron rich nuclei, in particular, those with loosely bound neutrons can give a very specific and unique way to measure the neutron distribution. In a previous paper [1] we have obtained the values of the hfs anomaly calculated in a two-body core + neutron model for the ^{9,11}Be isotopes. The hfs anomaly ϵ is defined as the sum of the hfs anomaly related to the Bohr-Weisskopf effect (ϵ_{BW})[2] and of the Breit-Rosenthal-Crawford-Shawlow (BRCS) correction δ [3], $\epsilon = \epsilon_{BW} + \delta$.

It was found in Ref.[1] that in Be isotopes, the value ϵ_{BW} is comparable to the BRCS correction δ. The value ϵ_{BW} is very sensitive to the weights of the partial states in the ground state wave function and might vary within 50% depending on those weights. In [1], we found a difference of about 25% for the total hfs anomaly value in the ^{9,11}Be isotopes.

In the present paper, we calculate the hfs anomaly in a three-cluster model of ^{9}Be and study the sensitivity of the hfs anomaly to the clusterization effects. The calculations are performed with two different three-body wave functions [4, 5]. These wave functions differ from each other by the choice of the cluster-cluster interaction potentials used in their calculations. They are characterized by the same partial states but contributing with different weights. They both reproduce the ^{9}Be rms radius and the three-cluster ($\alpha+\alpha+n$) dissociation energy (1.573 MeV). We compare the results obtained with these two wave functions, and also compare the present results with the core + neutron model calculations [1, 6].

The accuracy of the description of the ^{9}Be ground state wave function can be explored by calculating the magnetic dipole and electric quadrupole moments which are determined by the weights and quantum numbers of the states. The ^{9}Be magnetic dipole moment is independent of the radial behavior of the wave function but this is not the case for the electric quadrupole moment. Calculation of both the magnetic dipole and electric quadrupole moments thus provides a precise test of the accuracy of all aspects of the ground state wave function (for the experimental data on the magnetic dipole moment in the Be isotopes, we refer to Refs. [7], [8]; no experimental data exists on the hyperfine anomaly for these nuclei). We also compare the results for ^{9}Be$^+$ to that for ^{11}Be$^+$, to investigate the sensitivity of the hfs anomaly to diffuse (halo)neutron structures.

II. THREE-BODY WAVE FUNCTION

The wave function Ψ^{3b}_{JM} of the fragment relative motion in the three-cluster model ($\alpha+\alpha+n$) of ^{9}Be is described with the Jacobi coordinates in the method of hyperspherical harmonics [9, 10]. It is written as

$$\Psi^{3b}_{JM}(\xi_{\mathbf{1}},\xi_{\mathbf{2}}) = \sum_{KLSS_xl_1l_2M_L} [F^{KSS_xl_1l_2}_{LM_L} \otimes \chi^{s_1(s_2s_3)S_x}_{SM-M_L}]^{JM},$$

where $F^{KSS_xl_1l_2}_{LM_L}$ is the "active part" of the three-body wave function carrying the total orbital angular momentum L with the projection M_L. χ_{SM_S} is the total spin function of the whole system with the total spin S and projection M_S (here restricted to the neutron spin function). The wave function $F^{KSS_xl_1l_2}_{LM_L}(\xi_1,\xi_2)$ depends on the relative coordinates (hyperradius and relative angles) and the neutron spin

$$F^{KSS_xl_1l_2}_{LM_L}(\xi_1,\xi_2) = \rho^{-5/2}\Re^{LSS_x}_{Kl_1l_2}(\rho)\Im^{l_1l_2}_{KLM_L}(\Omega_5),$$

where l_1 and l_2 are the angular momenta of the relative motion corresponding to the ξ_1 and ξ_2 coordinates. The sum $\vec{L} = \vec{l_1} + \vec{l_2}$ gives the total angular momentum; K is the hypermomentum.

The hyperradius $\rho^2 = \xi_1^2 + \xi_2^2$ is a collective rotationally and permutationally invariant variable, ξ_1 and ξ_2 are the

*Electronic address: Yulia.Parfenova@ulb.ac.be; Also at Skobeltsyn Institute of Nuclear Physics, Moscow State University, 119992 Moscow, Russia.
†Electronic address: cwillain@ulb.ac.be

translationally invariant normalized sets of Jacobi coordinates. We choose the Jacobi coordinates as follows:

$$\begin{aligned} \mathbf{x} &= (A_{23})^{1/2}\mathbf{r_{23}}, \\ \mathbf{y} &= (A_{1(23)})^{1/2}\mathbf{r_{1(23)}}, \end{aligned} \quad (1)$$

where $\mathbf{r_{23}}$ is the relative coordinate of fragments 2 and 3, and $\mathbf{r_{1(23)}}$ is the coordinate of fragment 1 relative to the center of mass of the fragments 2 and 3. A_{23} is the reduced mass number for the pair (2,3), similarly, $A_{1(23)}$ is the reduced mass of the fragment 1 with respect to the mass of the subsystem $(2,3)$.

The five hyperspherical polar angles are $\Omega_5 = \{\theta, \hat{x}, \hat{y}\}$ where θ is defined by the relations

$$\begin{aligned} \xi_1 \equiv x &= \rho \sin\theta, \\ \xi_2 \equiv y &= \rho \cos\theta. \end{aligned} \quad (2)$$

The choice of three different systems of Jacobi coordinates leads to three-body wave functions with different phase factor, the three different Jacobi coordinates systems being connected together by defined rotations. For ^{9}Be, the T-basis correspond to choose the neutron as fragment 1, the two α-particles as fragments 2 and 3. The Y-basis associates the fragment 1 with one of the α-particles.

The values of the hypermomentum are $K = l_x + l_y + 2n$ $(n = 1, 2, ...)$. The hyperspherical harmonics have the form

$$\Im^{l_x l_y}_{K L M_L}(\Omega_5) = \psi^{l_x l_y}_K(\theta)[Y_{l_x}(\hat{x}) \otimes Y_{l_y}(\hat{y})]_{L M_L},$$

where

$$\psi^{l_x l_y}_K(\theta) = N^{l_x l_y}_K (\sin\theta)^{l_x} (\cos\theta)^{l_y} P^{l_x+1/2, l_y+1/2}_n(\cos 2\theta)$$

and $P^{\alpha,\beta}_n$ is a Jacobi polynomial. $N^{l_x l_y}_K$ is the coefficient of normalization

$$N^{l_x l_y}_K = \sqrt{\frac{2(n!)(K+2)(n+l_x+l_y+1)!}{\Gamma(n+l_x+3/2)\Gamma(n+l_y+3/2)}}$$

and the normalization condition for the function $\psi^{l_x l_y}_K(\theta)$ is

$$\int_0^{\pi/2} \psi^{l_x l_y}_K(\theta)\psi^{l'_x l'_y}_{K'}(\theta) \sin^2\theta \cos^2\theta d\theta = \delta_{KK'}\delta_{l_x l'_x}\delta_{l_y l'_y}.$$

The charge density distribution of the three-body nucleus entering the calculation of the electronic wave functions can be obtained as

$$\rho(\mathbf{r}) = \rho_{\mathbf{0}} < \mathbf{\Psi^{3b}_{JM}} \left| \sum_{\mathbf{i}} \mathbf{Z_i}\rho_{\mathbf{i}}(\mathbf{r}, \mathbf{x}, \mathbf{y}) \right| \mathbf{\Psi^{3b}_{JM}} >, \quad (3)$$

where ρ_0 is a normalization factor. In the case of ^{9}Be, the α-particle density distribution is approximated by a sum of Gaussians, with the parameters taken from [11] and giving a charge radius equal to 1.676 fm.

In the proceeding calculations two differing evaluations of Ψ^{3b}_{JM} [4, 5] as noted in Section I are used.

III. MAGNETIC HYPERFINE STRUCTURE

Here, we briefly mention the main points of the formalism for the hfs anomaly calculations. For more details we refer to [1] and references therein.

The magnetic hyperfine interaction Hamiltonian is defined by

$$\mathcal{H} = -\int \mathcal{J}(\mathbf{r}) \cdot \mathbf{A}(\mathbf{r})\, \mathbf{d^3 r}, \quad (4)$$

where $\mathcal{J}$ is the nuclear current density and $\mathbf{A}$ is the vector potential created by the atomic electrons.

The hyperfine interaction couples the electronic angular momentum $\mathbf{J}$ and the nuclear one $\mathbf{I}$ to a hyperfine momentum $\mathbf{F} = \mathbf{J} + \mathbf{I}$. The magnetic hyperfine splitting energy W for a state $\mid IJFM_F = F >$ is defined as the matrix element of the Hamiltonian $\mathcal{H}$.

The functions $F^{\kappa J}$, $G^{\kappa J}$ entering the matrix element are the radial parts of the large and small components of the Dirac electronic wave function, with the quantum number $\kappa = \pm(J + \frac{1}{2})$ for $J = l_e \mp \frac{1}{2}$ and the orbital angular momentum l_e. The calculations are preformed with a realistic electronic wave function (see [1]).

The magnetic dipole contribution to the hyperfine splitting $W_{(IJ)FF}$ has the form

$$\begin{aligned} W_{(IJ)FF} &= < IJFF|\mathcal{H}|IJFF > \\ &= \frac{1}{2}[F(F+1) - I(I+1) - J(J+1)]a_I, \end{aligned} \quad (5)$$

where a_I is defined as

$$a_I = -\frac{2e\kappa\mu_N}{IJ(J+1)} < II \mid \sum_{i=1}^{A} (M^{l_i}_Z(\mathbf{r}_i) + M^{s_i}_Z(\mathbf{r}_i)) \mid II >$$

with the Z components of the magnetic dipole moment $\mathbf{M}^{l_i(s_i)}(\mathbf{r}_i)$, related to the angular momentum l_i and spin s_i of each nucleon; the summation runs over all the nucleons.

For an extended nuclear charge we have

$$\begin{aligned} \mathbf{M}^l(\mathbf{r}_i) &= g^i_l \mathbf{l}_i [\int_{r_i}^{\infty} F^{\kappa J} G^{\kappa J}\, dr + \int_0^{r_i} F^{\kappa J} G^{\kappa J} (\frac{r}{r_i})^3 dr], \\ \mathbf{M}^s(\mathbf{r}_i) &= g^i_s \mathbf{s}_i \int_{r_i}^{\infty} F^{\kappa J} G^{\kappa J} dr + \mathbf{D}_i \int_0^{r_i} F^{\kappa J} G^{\kappa J} (\frac{r}{r_i})^3 dr, \end{aligned}$$

with $\mathbf{D}_i = -\sqrt{\frac{5}{2}}\left[\mathbf{s}^1 \otimes C^2(\hat{r}_i)\right]^1$ and $C^k_q = \sqrt{\frac{4\pi}{2k+1}} Y_{kq}(\hat{r}_i)$.

The quantity a_I can be expressed through the hfs constant for a point nucleus $a^{(0)}_I$ as

$$a_I \approx a^{(0)}_I (1 + \epsilon_{BW} + \delta), \quad (6)$$

with

$$a^{(0)}_I = -\frac{2e\kappa\, \mu_N \mu}{IJ(J+1)} \int_0^{\infty} F^{\kappa J}_0(r) G^{\kappa J}_0(r) dr. \quad (7)$$

Here, $\mu =< II \mid \sum_{i=1}^{A}(g_s^i s_i + g_l^i l_i) \mid II >$ defines the magnetic dipole moment of the point nucleus in nuclear magneton units μ_N. The functions $F_0^{\kappa J}$, $G_0^{\kappa J}$ are the radial parts of the Dirac electronic wave function in the point nucleus approximation.

The hfs anomaly in the Bohr-Weisskopf effect is

$$\epsilon_{BW} = -\frac{b}{\mu}\sum_{i=1}^{3}\left[\sum_{j=1}^{n_i}\Big\{< II|(g_s^{(j)}s_j + g_l^{(j)}l_j)K^a(r_j)|II > - < II|(g_l^{(j)}l_j + D_j)K^b(r_j)|II >\Big\}\right], \quad (8)$$

where $b = [\int_0^\infty F_0^{\kappa J}G_0^{\kappa J}dr]^{-1}$, and

$$K^a(r_j) = \int_0^{r_j} F^{\kappa J}G^{\kappa J}dr, \quad (9)$$

$$K^b(r_j) = \int_0^{r_j} F^{\kappa J}G^{\kappa J}(\frac{r}{r_j})^3 dr. \quad (10)$$

The index j is related to the A nucleons; $i(1-3)$ denotes one of the three-clusters of n_i nucleons. $g_l^{(j)}$ and $g_s^{(j)}$ are the gyromagnetic ratios of the j-th nucleon orbital motion and spin, respectively.

The hfs anomaly can be approximated by

$$\epsilon_{BW} = -\frac{b}{\mu}\sum_{i=1}^{3}\left[\Big\langle II|(g_s^{(i)}s_i + g_l^{(i)}l_i)K^a(r_i)|II\Big\rangle - \Big\langle II|(g_l^{(i)}l_i + D_i)K^b(r_i)|II\Big\rangle\right]. \quad (11)$$

The index i is related to the three-clusters of relative coordinate r_i and angular momentum l_i in respect to the center of mass system, and with the appropriated expressions $g_s^{(i)}, g_l^{(i)}$ and D_i, calculated for each cluster. The BRCS correction is defined as $\delta = 1 - bK^a(\infty)$ [3]. This term is defined by the nuclear charge distribution and information on the neutron distribution is contained solely in ϵ_{BW}.

IV. HFS ANOMALY AND NUCLEAR MOMENTS OF ^{9}BE IN THE CLUSTER MODEL

To calculate the magnetic dipole moment and the hfs anomaly, we use three systems of coordinates related to each other by rotation: the T-basis with the neutron as cluster $i = 1$, and the $Y(q)$ systems ($q = 1$ or 2) with one of the α-particles as cluster $i = 2$ or 3. The index $q = 1$ and $q = 2$ define respectively the rotations $1(23) \rightarrow 2(31)$ and $1(23) \rightarrow 3(12)$ between the T and Y-basis.

The transformation of the hyperspherical harmonic function [10] from the T-basis to the Y-basis is defined by

$$\Im^{l_x l_y}_{KLM_L}(\Omega_5) = \sum_{l'_x l'_y}\left\langle l'_x l'_y|l_x l_y\right\rangle^q_{KL}\Im^{l'_x l'_y}_{KLM_L}(\Omega'_5), \quad (12)$$

where $\left\langle l'_x l'_y|l_x l_y\right\rangle^q_{KL}$ are the Raynal-Revai coefficients [10].

The transformation of the spin part of the wave function is written as

$$\chi^{s_1(s_2 s_3)S_x}_{SM_S} = \sum_{S'_x}\langle S'_x|S_x\rangle^q_S\,\chi^{s'_1(s'_2 s'_3)S'_x}_{SM_S} \quad (13)$$

with $s'_1 = s_{2(3)}$, $s'_2 = s_{3(1)}$, and $s'_3 = s_{1(2)}$ for $q = 1(2)$,

$$\langle S'_x|S_x\rangle^q_S = (-)^{s_{1(2)}+2s_{2(1)}+s_3+S'_x(S_x)}\hat{S}_x\hat{S}'_x \times \begin{Bmatrix} s_{2(3)} & s_{3(2)} & S_x \\ s_1 & S & S'_x \end{Bmatrix}, \quad (14)$$

where $\mathbf{S} = \mathbf{s_2} + \mathbf{s_3} + \mathbf{s_1}$, $\mathbf{S_x} = \mathbf{s_2} + \mathbf{s_3}$, and $\mathbf{S'_x} = \mathbf{s_{3(1)}} + \mathbf{s_{1(2)}}$.

To calculate the magnetic dipole moment, we consider the contribution of each fragment with respect to the rest system. In ^{9}Be, the neutron spin and the α-particle orbital motion contribute to the magnetic dipole moment as

$$\mu = \sum_{\varsigma}\omega_\varsigma^2\,\langle m_s\rangle\, g_s^{(n)} + \frac{5}{9}\sum_{q=1,2}\sum_{\varsigma'}\beta^2_{\varsigma'}\,\langle m_y\rangle_q\, g^{(\alpha)}_{l'_y}. \quad (15)$$

$\langle m_s\rangle, \langle m_y\rangle_q$ are the expectation values of the spin and angular momentum projections of the fragments. $\langle m_s\rangle$ is found in the T-basis and associated with the neutron spin; $\langle m_y\rangle_q$ is found in the Y-basis obtained by the rotation $q = 1(2)$ for $i = 2(3)$ (see (12) and (13)) and associated with the α-particle orbital momentum. In Eq. (15) ω_ς^2 is the weight of the partial state in the T-basis for the channel with quantum numbers $\varsigma = Ll_x l_y$; and $\beta^2_{\varsigma'}$ is the weight of the partial state obtained with (12) and (13) for each channel with quantum numbers $\varsigma' = Ll'_x l'_y$ in the Y-basis. Here, we mean by channel the set ς of quantum numbers characterizing the partial waves contributing to the ground state wave function. In the case of ^{9}Be represented by the system $\alpha + \alpha + n$, this set of quantum numbers is L, l_x, and l_y defined in Section II. The nuclear wave function is summed over the hypermomentum K which is not included explicitly as the matrix element does not depend on it.

In Eq. (15), $\mu_n = \frac{1}{2}g_s^{(n)}$ denotes the magnetic dipole moment of the neutron and $\mu^\alpha_{l'_y} = g^{(\alpha)}_{l'_y}m_y = 2\frac{A_1+A_2}{AA_3}g^{(p)}_{l_y}m_y$ is the magnetic dipole moment of the α-particle in the state with l_y as angular momentum in the Y-basis. Note that the magnetic dipole moments are obtained using for the g factors $g_s^{(n)} = -3.8260854(90)$ and $g^{(p)}_{l_y} = 1$.

The factor $\frac{5}{9}$ in (15) is the center of mass factor $\frac{A-A_{2(3)}}{A}$ in the Y-basis corresponding to the $\alpha + (\alpha + n)$ system.

We assume that the α-particle angular momentum is defined by two orbiting protons, neglecting the spin contribution of the nucleons.

The electric quadrupole moment is

$$Q = 2\sum_{i=1}^{3} \left\langle II|r_i^2 C_0^2(\hat{r}_i)|II\right\rangle, \tag{16}$$

where the summation runs over the fragments.

In the three-cluster model of ^{9}Be, the hfs anomaly in the Bohr-Weisskopf effect is found as the weighted sum

$$\begin{aligned}\epsilon_{BW} &= -\frac{b}{\mu_I}\left\{\sum_{\varsigma}\omega_\varsigma^2 \langle m_s\rangle g_s^{(n)}\right. \\ &\times \left[K_\varsigma^a - K_\varsigma^b\left(1 \mp \frac{6}{4}\frac{2I+1}{2(I+1)}\right)\right] \\ &+ \left.\frac{5}{9}\sum_{q=1,2}\sum_{\varsigma'}\beta_{\varsigma'}^2 \langle m_y\rangle_q g_{l_y'}^{\alpha}\left[K_{\varsigma'}^a - K_{\varsigma'}^b\right]\right\},\end{aligned} \tag{17}$$

where the sign $\mp$ corresponds to $I = l_y \pm \frac{1}{2}$, and where μ is replaced by the experimental value ($\mu_I = -1.1778(9)\mu_N$ [7]) of the ^{9}Be magnetic dipole moment.

Here we denote

$$K_\varsigma^a = \int_0^\infty |\Phi_\varsigma(R)|^2 K^a(\frac{A-A_i}{A}R)R^2 dR \tag{18}$$

$$K_\varsigma^b = \int_0^\infty |\Phi_\varsigma(R)|^2 K^b(\frac{A-A_i}{A}R)R^2 dR \tag{19}$$

where the ratio $\frac{A-A_i}{A}$ takes into account the center of mass motion, A_i is the valence fragment mass (the neutron mass ($i=1$) in the T-basis, and the α-particle mass ($i=2,3$) in the Y-basis).

So, we can write

$$\epsilon_{BW} = \sum_\varsigma \omega_\varsigma^2 \epsilon_{BW}^\varsigma \tag{20}$$

where ϵ_{BW}^ς is obtained for each channel $|\varsigma>$.

V. RESULTS AND DISCUSSION

1. *Three-body model of ^{9}Be*

In the calculations we use two ground state wave functions of the ^{9}Be described as the three body $\alpha+\alpha+n$ system. These wave functions are obtained with different $\alpha-\alpha$ and $\alpha-n$ interaction potentials.

The first wave function, WF1 [4], is obtained with supersymmetric equivalent potential [14]. With the α-particle charge radius 1.676 fm [11] this wave function gives the value 2.564 fm for the ^{9}Be charge rms radius. This value agrees with the experimental ones, 2.519(12) and 2.50(9) fm (see [11] and references therein). The ^{9}Be magnetic dipole moment $\mu_{^9Be} = -1.0531\mu_N$ is less by 10% compared to the experimental values, $-1.177432(3)\mu_N$ [15] and $-1.1778(9)\mu_N$ [7]. The calculated electric quadrupole moment is 53.39 mb which is in good agreement with the experimental value 52.88(38) mb [16].

The second wave function, WF2 [5], is obtained with the Ali-Bodmer potential [17] and the α-neutron interaction potential [18]. The three-body interaction potential is adjusted to fit the three-cluster dissociation energy 1.573 MeV. The value of the ^{9}Be charge radius, 2.707, fm is overestimated compared to the experimental one. The ^{9}Be magnetic dipole moment $\mu_{^9Be} = -1.316\mu_N$ is 10% larger than the experimental value. The electric quadrupole moment is $Q = 65.42$ mb.

The difference between these wave functions is in the radial y dependence of the valence neutron wave function (obtained by integration over the x coordinate and the angles), the core charge radius and the weights of the partial states L, l_x, l_y for the ground state wave function (see Tables I and II).

TABLE I: The weights of the partial waves $\omega^2_{Ll_xl_y}$, the mean ^{8}Be-neutron distance r_n, the neutron contribution $\epsilon_{BW}^{\varsigma(n)}$ to the values of the hfs anomaly obtained with WF1.

ς Ll_xl_y	ω_ς^2	r_n fm	$\epsilon_{BW}^{\varsigma(n)}$ %
101	0.498355	3.274	-0.0332
121	0.315975	3.159	-0.0229
221	0.152790	2.976	0.0123
123	0.019661	3.758	-0.0312
223	0.003674	3.585	-0.0286
143	0.006608	3.689	-0.0303
243	0.001595	4.397	0.0245

TABLE II: The same as in Table I calculated with the wave function WF2.

ς Ll_xl_y	ω_ς^2	r_n fm	$\epsilon_{BW}^{\varsigma(n)}$ %
101	0.592607	3.778	-0.0402
121	0.286695	3.381	-0.0248
221	0.090244	3.284	0.0141
123	0.020740	3.870	-0.0313
223	0.002710	3.753	-0.0296
143	0.005362	3.770	-0.0299
243	0.001154	3.760	0.0179

Tables I and II show the neutron contribution $\epsilon_{BW}^{\varsigma(n)}$ to the hfs anomaly (first term in (17)) and the root mean square distance of the valence neutron r_n from the ^{8}Be center of mass in each channel ς.

The contributions to the hfs anomaly in the Bohr-Weisskopf effect, $\epsilon_{BW}^{(n)}$ and $\epsilon_{BW}^{(\alpha)}$, and the BRCS correction δ calculated with WF1 and WF2 are listed in Table III.

The contribution of the hfs anomaly from the α-

TABLE III: The ^{9}Be charge rms radius, the neutron radial distance r_n, the contributions to the hfs anomaly from the neutron spin ($\epsilon^{(n)}_{BW}$) and from the α-particle orbital motion ($\epsilon^{(\alpha)}_{BW}$), the values of ϵ_{BW} and of δ calculated for the two wave functions $WF1,2$ (α-particle radius: 1.676 fm) are compared to the (core+neutron) results. WF2* refers to another choice of the α-particle radius (1.46 fm).

Value	core+neutron	WF1	WF2	WF2*
rms (fm)	2.519	2.564	2.707	2.533
r_n (fm)		3.207	3.621	
$\epsilon^{(n)}_{BW}$ (%)		-0.02281	-0.03059	
$\epsilon^{(\alpha)}_{BW}$ (%)		0.00085	0.00088	
ϵ_{BW} (%)	-0.0236	-0.02112	-0.02882	-0.03032
δ	-0.0451	-0.04644	-0.04926	-0.04634
ϵ	-0.0687	-0.06756	-0.07809	-0.07666

particle orbital motion, $\epsilon^{(\alpha)}_{BW}$ (second term in (17)) is small compared to that from the neutron, $\epsilon^{(n)}_{BW}$; and its variation is small also (see Table III).

To explore the sensitivity of the results to the charge radius of the α-clusters in ^{9}Be, we vary the value of the α-particle charge radius from 1.676 to 1.636 fm. The last value of the charge radius is obtained with regard to the negative contribution of the neutron charge distribution, $(0.34)^2$ fm^2 (see [19, 20]).

Correspondingly, the ^{9}Be charge radius changes from 2.564 to 2.534 fm for WF1 and from 2.707 to 2.678 fm for WF2. Owing to the radial behavior of the electronic wave functions (see Fig. 1) entering the expressions (9), (10), and (17)-(19), with a smaller charge radius (rms and rms$_C$) we get a larger value of the hfs anomaly in the Bohr-Weisskopf effect. Thus, in our case, we get an increase in the hfs anomaly value ϵ_{BW} by 1.6% for WF1 and 0.5% for WF2.

The α-α distance is smaller when calculated with WF1, so correspondingly, the ^{9}Be charge radius is smaller and the value of the BRCS correction δ is less (see Table III). δ varies within 6% depending on the description of the nuclear wave function.

ϵ_{BW} and the total hfs anomaly ϵ which is the sum $(\epsilon^{(n)}_{BW} + \epsilon^{(\alpha)}_{BW} + \delta)$, are mainly determined by the neutron distribution. There is no direct correspondence of the hfs anomaly value to the nuclear charge radius. For example, if we put the radius of the α-particle at 1.46 fm, the ^{9}Be charge radius obtained with WF2 is 2.533 fm and the hfs anomaly ϵ=-0.07666% (see Table III WF2*). These values are larger than those obtained with WF1 with the charge radius 2.564 fm. Thus, even with smaller charge radius values one can get larger values of ϵ_{BW} and ϵ.

Therefore, we can conclude that the hfs anomaly is more sensitive to the neutron spatial distribution than to the charge distribution of the whole nucleus, and the value r_n is a crucial parameter for the hfs value in the Bohr-Weisskopf effect.

With the different nuclear wave functions, the r_n value varies of about 10% and the hfs anomaly ϵ_{BW} of about 30%. As the value of the hfs anomaly ϵ_{BW} is about two times smaller than δ,the total hfs anomaly ϵ varies within 14% with the choice of the wave function.

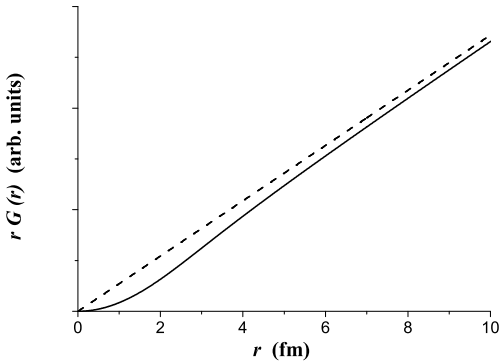

FIG. 1: The electronic wave functions obtained for the distributed nuclear charge, G (dashed line), and for the point nuclear charge, G_0 (solid line).

We should also mention that the value of the hfs anomaly is very sensitive to the contribution of the different partial states in the ^{9}Be ground state wave function. In particular, the hfs anomaly $\epsilon^{(n)}_{BW}$ in the channels $\varsigma = 121$ and $\varsigma = 221$ (that is of 50% of the nuclear wave function) is twice as small as $\epsilon^{(n)}_{BW}$ in the channel $\varsigma = 101$. Thus, the relative weights of these states are of major importance. As found in [21] the magnetic dipole moment in the $\alpha + \alpha + n$ cluster model is also rather sensitive to these weights. In the case of ^{9}Be, three channels mostly contribute to the magnetic dipole moment and the hfs anomaly, $\varsigma = 101$, $\varsigma = 121$, and $\varsigma = 221$. The magnetic dipole moment in this case is [21]

$$\mu \approx -1.857\omega^2_{101} - 1.191\omega^2_{121} + 1.914\omega^2_{221} + \mu_{res}. \quad (21)$$

According to [21] the experimental magnetic dipole moment value can be reproduced under the condition $\omega^2_{221} < 16$ %. Otherwise the calculated value is underestimated.

Let us analyze the correlation between the weights and the values of the ^{9}Be hfs anomaly, magnetic dipole and electric quadrupole moments, noting that the analysis is model dependent.

To estimate how the hfs anomaly $\epsilon^{(n)}_{BW}$ varies with the weights of the different states, we consider the contributions of these three channels only (so that $\omega^2_{101} + \omega^2_{121} + \omega^2_{221} + \omega^2_{res} = 1$) and find the weights satisfying the experimental value of the ^{9}Be magnetic dipole moment ($\mu_I = -1.177432(3)\mu_N$). Under this condition, we get the hfs anomaly value plotted in Fig. 2 as a function of ω^2_{101} for the wave functions WF1 and WF2 (solid and dashed lines, respectively).

Similarly one can express the electric quadrupole moment through the weights of these dominant states. For

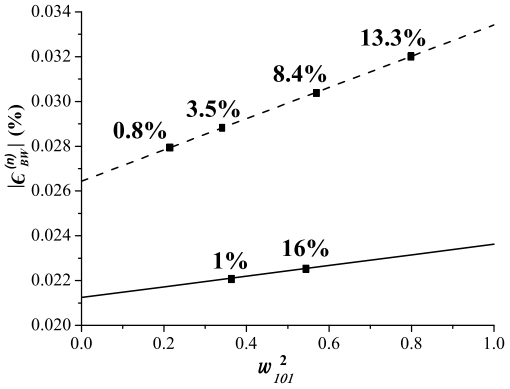

FIG. 2: The variation of the Bohr-Weisskopf hfs anomaly value from the neutrons with the weight ω^2_{101} for WF1 (solid line) and WF2 (dashed line)(α-particle radius: 1.676 fm). The dots on the lines are the values in agreement with the electric quadrupole moment(see text). The weight ω^2_{221} is indicated for each point.

WF1 we get

$$\begin{aligned} Q &\approx 3.157\omega^2_{101} - 4.553\omega^2_{121} - 4.527\omega^2_{221} \\ &+ 2\omega_{101}\omega_{121}32.859 + 2\omega_{101}\omega_{221}32.039 + \\ &+ 2\omega_{121}\omega_{221}7.314 + Q_{res}, \end{aligned} \quad (22)$$

where $Q_{res} = 11.97$ mb.

For WF2 this relation is

$$\begin{aligned} Q &\approx 4.204\omega^2_{101} - 6.635\omega^2_{121} - 6.662\omega^2_{221} \\ &+ 2\omega_{101}\omega_{121}41.908 + 2\omega_{101}\omega_{221}41.610 \\ &+ 2\omega_{121}\omega_{221}9.918 + Q_{res}, \end{aligned} \quad (23)$$

where $Q_{res} = 13.11$ mb.

ω^2_{res}, μ_{res} and Q_{res} are the contributions of the neglected channels respectively to the weights, the magnetic dipole and electric quadrupole moments. The square dots on the lines in Fig. 2 point the hfs values obtained with the weights which also satisfy the experimental value of the ^{9}Be electric quadrupole moment 52.88(38) mb. For each wave function we get a few points - two for WF1 or even four for WF2. On this figure we also report the corresponding values of the weight ω^2_{221} ($\omega^2_{221} < 16\%$). One can see the ranges of the hfs anomaly values obtained with WF1 and WF2 respectively Therefore, an experimental estimation of the hfs anomaly in the Bohr-Weisskopf effect could give values for the weights of the partial states in the ground state wave function.

The figure shows that the hfs anomaly is a very critical quantity to test the nuclear wave function, all other parameters being equivalently well described, in particular, the electronic part.

2. Comparison with the core+neutron model

In Ref. [1], the hfs anomaly for ^{9}Be was calculated within the core+neutron model of ^{9}Be. The ^{9}Be ground state wave function was given by the superposition of states

$$\begin{aligned} \left|^9\mathrm{Be}\left(3/2^-\right)\right\rangle &= \omega_{0^+}\left|\left[^8Be\left(0^+\right)\otimes n_{p_{3/2}}\right]_{3/2^-}\right\rangle \\ &+ \omega_{2^+}\left|\left[^8Be\left(2^+\right)\otimes n_{p_{3/2}}\right]_{3/2^-}\right\rangle. \end{aligned} \quad (24)$$

corresponding to the ^{8}Be core in the ground (0^+) and excited (2^+) states with the neutron separation energies 1.665 and 4.705 MeV, respectively.

With the weights $\omega^2_{0^+} = 0.535$ and $\omega^2_{2^+} = 0.465$ obtained with the spectroscopic factors from Ref. [22] the magnetic dipole moment is $\mu = -1.0687\ \mu_N$ and ϵ_{BW}, δ and ϵ have the values reported in Table III. The ϵ_{BW} is close to the values $\epsilon_{BW} = -0.0249\%$ [6] (obtained with the weights $\omega^2_{0^+} = \omega^2_{2^+} = 0.5$) and $\epsilon_{BW} = -0.0243\%$ from [23].

The ϵ_{BW} values obtained for the 0^+ state in the (core+neutron) model ($\epsilon_{BW} = -0.0440\%$) and for the $l_x = 0$ state of $WF1$ or $WF2$ in the $(\alpha+\alpha+n)$ model ($\epsilon_{BW} = -0.0332\%$ or -0.0402%) are relatively close to each other. On the contrary, the ϵ_{BW} values for the different partial states $l_x = 2$ in the three cluster model exceed by a few times (see Tables I and II) the value obtained for the 2^+ state in the (core + neutron) model ($\epsilon_{BW} = -0.0063\%$).

The BRCS correction obtained with the two-body wave function is -0.0451%, close to that obtained in the three-body calculations. Thus in the core+neutron model we get $\epsilon = -0.0687\%$, to be compared with the values $\epsilon = -0.06756\%$ and $\epsilon = -0.07809\%$ obtained with the three clusters $\alpha+\alpha+n$ wave functions.

Thus the clustering effect, revealing itself in the set of states contributing to the ground state wave function, lead to a variation of the hfs value ϵ of less than 2% for WF1 and of about 14% for WF2. Compared to the ^{11}Be nucleus the difference in the value of the hfs anomaly in the Be isotopes is about 25%. This value gives us the accuracy of the measurements of the hfs anomaly needed to study clustering effects in light nuclei.

This results corroborates the conclusion in Ref. [6], that the value of the hfs anomaly reflects the extended neutron distribution in ^{11}Be and might indicate a neutron halo, but the difference for the different isotopes is not so pronounced as was found in Ref. [6].

VI. CONCLUSION

In the present paper, we have calculated the hfs anomaly in the ^{9}Be$^+$ ion with the nucleus described in a three-cluster model. The $1s^22s$ electronic wave function is obtained taking into account the charge distribution of the clustered $(\alpha+\alpha+n)$nucleus and the shielding effect of two electrons in the $1s^2$ configuration.

The result of the calculations strongly depends on the weights of the partial waves contributing to the ground state wave function. Together with the magnetic dipole and electric quadrupole moments the value of the hfs anomaly can be used to study the clustering effects in neutron rich light nuclei.

The total hfs anomaly is the sum of δ and ϵ_{BW}. The BRCS correction δ is only determined by the nuclear charge distribution and slightly varies from isotope to isotope. The value of the BRCS correction is comparable or larger than the value of ϵ_{BW}. The hfs anomaly in ^{11}Be differs from that in ^{9}Be by 25%. The clustering effect leads to variations of the hfs value within 15%. The calculated magnitude and differential change in the value of the hfs anomaly is indicative of the experimental precision that must be achieved to study the clustering effect and the neutron distribution in neutron rich light nuclei.

VII. ACKNOWLEDGMENTS

The authors are grateful to Dr P. Descouvemont and Dr. L.V. Grigorenko for helpful discussions and for having provided the numerical values of the wave functions they have calculated for ^{9}Be in a three-body model.

This paper has been supported by the Belgian Program P5-07 of Inter-university Attraction Poles initiated by the Belgian-state Federal Services for Scientific Politics. Y.L.P. has received an one year postdoctoral research grant from the Cooperation of the Belgian Scientific Politics with Central and Oriental European countries.

[1] Y.L. Parfenova and C. Leclercq-Willain, APS-123-QED, Feb 2005. 9pp. e-Print Archive: nucl-th/0502032 Accepted in Phys. Rev. **C**, June (2005).
[2] A. Bohr and V.F. Weisskopf, Phys. Rev. **77**, 94 (1950).
[3] H.J. Rosenberg and H.H. Stroke, Phys. Rev. **A5**, 1992 (1972).
[4] Private Communications *Three clusters approach of the ^{9}Be ground state wave function* **WF1**: P. Descouvemont, Physique nucléaire théorique et Physique Mathématique, U.L.Bruxelles, Bruxelles, Belgium. pdesc@ulb.ac.be
[5] L.V. Grigorenko, R.C. Johnson, I.G. Mukha, I.J. Thompson, M.V. Zhukov, Eur. Phys. J. **A15**, 125 (2002)
[6] T. Fujita, K. Ito, and T. Suzuki, Phys. Rev. **C59**, 210 (1999).
[7] E. W. Weber and J. Vetter, Phys. Lett. **A56**, 446 (1976).
[8] W. C. Dickinson and T. F. Wimett, Phys. Rev. **75**, 1769 (1949).
[9] M. V. Zhukov, B. V. Danilin, D. V. Fedorov, J. M. Bang, I. J. Thompson, J. S. Vaagen, Phys. Rep. **231**, 151 (1993).
[10] Ya. A. Smorodinskii and V. D. Éfros, Yad. Fiz. **17**, 210 (1973) [Sov. J. Nucl. Phys. **17**, 107 (1973)].
[11] H. de Vries, C. W. de Jager, and C. de Vries, At. Data and Nucl. Data Tables **36**, 495 (1987).
[12] A.S.Davydov, "*Quantum Mechanics*", Pergamon Press, Oxford, London, Edinburg, New York, Paris, Frankfurt, 1965.
[13] M.E. Rose "*Relativistic Electron Theory*", John Wiley and Sons, New York, 1961.
[14] P. Descouvemont and C. Daniel, Phys. Rev. **C67**, 044309 (2003).
[15] W. M. Itano, Phys. Rev. **B27**, 1906 (1983).
[16] D. Sundholm and J. Olsen Chem. Phys. Lett. **177**, 91 (1991).
[17] D.V. Fedorov, A.A. Jensen, Phys. Lett. **B389**, 631 (1996).
[18] A. Cobis, D.V. Fedorov, A.S. Jensen, Phys. Rev. **C58**, 1403 (1998).
[19] I. Sick, Eur. J. Phys. A **24**, 65 (1999).
[20] G.S. Anagnostatos, A.N. Antonov, P. Ginis, J. Giapitzakis, M.K. Gaidarov, J. Phys. G: Nucl. Part Phys. A **24**, 69 (1999).
[21] V.T. Voronchev, V.I. Kukulin, V.N. Ponomarev, and G.G. Ryzhikh. Few Body Systems **18**, 191 (1995).
[22] S. Cohen and D. Kurath, Nucl. Phys. **A101**, 1 (1967).
[23] N. Yamanaka, Hyperfine interactions **127**, 129 (2000).